energies

Article

Efficient Demand Side Management Using a Novel Decentralized Building Automation Algorithm

Christodoulos Spagkakas, Dimitrios Stimoniaris and Dimitrios Tsiamitros *

Department of Electrical and Computer Engineering, School of Engineering, University of Western Macedonia, 50100 Kozani, Greece; dece00038@uowm.gr (C.S.); dstimoniaris@uowm.gr (D.S.)
* Correspondence: dtsiamitros@uowm.gr

Abstract: Given its adaptable and efficient energy consuming devices during peak hours, the residential building sector is urged to take part in demand response (DR) initiatives with the use of a building energy management system (BMS). The residents of buildings with BMS enjoy secure, pleasant, and fully managed lifestyles. Although the BMS helps the building consume less energy and encourages occupant engagement in energy-saving initiatives, unwelcome interruptions and harsh instructions from the system are inconvenient for the inhabitants, which further discourages their participation in DR initiatives. Building automation control is a crucial factor for improving buildings' energy efficiency and management, as well as improving the electricity grid's reliability indices. Smart houses that use the right sizing procedure and energy-management techniques can help lower the demand on the entire grid and potentially sell clean energy to the utility. Recently, smart houses have been presented as an alternative to traditional power-system issues including thermal plant emissions and the risk of blackouts brought on by malfunctioning bulk plants or transmission lines. This paper describes the necessary technology requirements and presents the methodology and the decentralized building automation novel algorithm for efficient demand side management in a building management system. Human comfort aspects including thermal comfort and visual comfort were taken into consideration when selecting heating and lighting controls. The suggested BMS relies primarily on a load-shifting technique, which moves controllable loads to low-cost periods to avoid high loading during peak hours. The model aims to minimize the individual household electricity consumption cost while considering customers' comfort and lifestyle. All these are applied in an experimental university microgrid, and the results are presented in terms of energy saving in kWh, money in €, and working hours. The results demonstrated that the proposed approach might successfully lower energy use during the DR period and enhance occupant comfort.

Keywords: smart grid; building automation; energy efficiency; energy management

check for updates

Citation: Spagkakas, C.; Stimoniaris, D.; Tsiamitros, D. Efficient Demand Side Management Using a Novel Decentralized Building Automation Algorithm. *Energies* **2023**, *16*, 6852. https://doi.org/10.3390/en16196852

Academic Editor: Vaidyanathan Krishnamurthy

Received: 22 August 2023
Revised: 15 September 2023
Accepted: 25 September 2023
Published: 27 September 2023

1. Introduction

The primary motivation for any energy management system is economic gain. Pricing systems define the appropriate characteristics of smart building management systems (BMSs), which have a substantial impact on the complexity and dependability of BMSs [1]. In order to promote the adoption of a BMS, some nations have already implemented a number of regulations, legislation, and subsidy programs, such as promoting heating system optimization, supporting energy storage infrastructure, and/or implementing smart meters. For instance, the integration of smart-home technology to reduce power demand in residential areas is encouraged by the European Standard EN 15232 [2] and the Energy Performance of Building Directive 2010/31/EU [3], which is in line with Directive 2009/72/EC and the Energy Road Map 2050 [4]. Power-grid authorities recently changed household electrical pricing to encourage proper demand-side control by homeowners. Furthermore, many countries support small-scale PV integration on residential or commercial rooftops and net metering [5,6]. The quick cut-off in these structures, however, might result in the breakdown, failure, or shortened lifespan of mechanical and electrical equipment, as well as their installations [7,8].

For DR participation, the BMS algorithm has been studied by several researchers [9–18]. They created optimization challenges to reduce the cost of energy and discomfort from heat for families [9–12,14,15], the physical and functional limitations of appliances [12], and the cost of electricity [13]. The creation of suitable input scenarios for the families and their load scheduling was the main focus of these investigations.

Even while these algorithms permit residents of the home to take part in DR programs, they are difficult to utilize for unidirectional and structured energy management. For instance, a unidirectional HEMS focused on reducing energy use annoys residents by forcing them to comply with severe rules for the use of building subsystems such as washing machines, refrigerators, and air conditioners.

Additionally, people who live in a house have a propensity to actively interact with their energy management system and any related systems.

Therefore, it is crucial to create a bi-directional BMS that adheres to the occupants' usage preferences for appliances and equipment as well as their behavioral patterns [13,19]. Control algorithms for home appliances, renewable energy sources, electric vehicles, and energy storage systems based on the quality of experience (QoE) were given for the BMS as one of the strategies to maintain the user's comfort and to lower the peak load and electricity cost of smart homes [20]. Although the DR programs were not taken into account in these experiments, the offered algorithms may nevertheless cover them.

On the other hand, RES-based electricity generation is unaffected by other conventional sustainable resources or variations in energy use. Sustainable generating is planned in accordance with expected load levels as well as some technological and environmental constraints. However, weather-dependent RES, such as PV facilities and wind farms, must run at maximum output whenever technically practicable in order to show a high proportion of RES in the electric energy production mixture. When considering limited or isolated energy networks (e.g., islands), these operating criteria cannot be met and may result in insufficient energy supply. Furthermore, as the proportion of renewable energy sources (RESs) in electricity generation grows, this problem becomes increasingly pressing.

All of the concerns listed above can be solved by integrating energy storage systems and controlled loads into the grid, as well as integrating enhancements to the control infrastructure and algorithms in a non-invasive manner for the distribution network. The microgrid, which is commonly characterized as a distribution grid incorporating distributed generators (DGs), energy storage units, and regulated loads [21], appears to be one of the most significant aspects of future power grid topologies. The auxiliary services that a microgrid's supply and demand sides could provide are predicted to improve the value of the future smart grid [22,23]. In general, load levelization and demand-side management are widely employed to provide services such as voltage regulation and energy management for isolated microgrids [24,25].

Because they are programmable, these authorized automation devices are typically put at the low-voltage sector of the grid and have numerous capabilities for controlling electric energy use. Their operation is based on a shared data bus, which allows simple binary signals to be transmitted to activate their varied capabilities. The accurate assessment and proper control of the State of Charge (SoC) of energy storage devices are critical during the islanded operation of microgrids [26,27]. According to [28], faulty control architecture and algorithms can have a severe impact on grid operation, resulting in an inaccurate SoC estimate as well as a decrease in customer power supply reliability. As a result, it is obvious that the control architecture of a smart distribution grid must be compatible and adequately interactive with energy storage devices and existing bus communication technologies.

The developers of [29] use the OPC server solution to address the issue of compatibility between the microgrid's control system and bus communication technologies. This technique has significant drawbacks, including a relatively expensive cost, the requirement of permanent additional hardware installation, and software version compatibility concerns.

Furthermore, in this scenario, the control algorithm of an experimental microgrid without bus technology, as described in [30], should be exposed to numerous changes. Because most DGs' principal energy sources (PV and wind) are stochastic in nature, incorporating weather prediction into microgrid control algorithms will be critical [23,24]; however, this is not a component of this paper.

In order to achieve optimal demand-side management, this paper describes the control infrastructure and algorithm of an experimental smart microgrid that is compatible with KNX bus systems [31–34] in a very simple and cost-effective manner. The first section describes the smart microgrid topology by emphasizing the unique control infrastructure components that transform the distribution network into a "smart grid" and the details of the suggested technique for integrating KNX bus devices into the microgrid; then, a brief overview of the microgrid's control method is offered, including its interoperability with KNX bus systems. Finally, the experimental results of the microgrid's operation are shown. According to the findings, incorporating smart cities (bus) systems might greatly improve consumer reliability performance and the supply/demand balance of microgrid-based smart grid topologies.

2. Materials and Methods

The experimental microgrid of UoWM is presented in Figure 1. Every DC load, generator, or energy storage device in a microgrid-based smart distribution grid architecture is equipped with individual DC–AC inverters and is connected to the AC microgrid via a KNX actuator and a multi tariff energy meter.

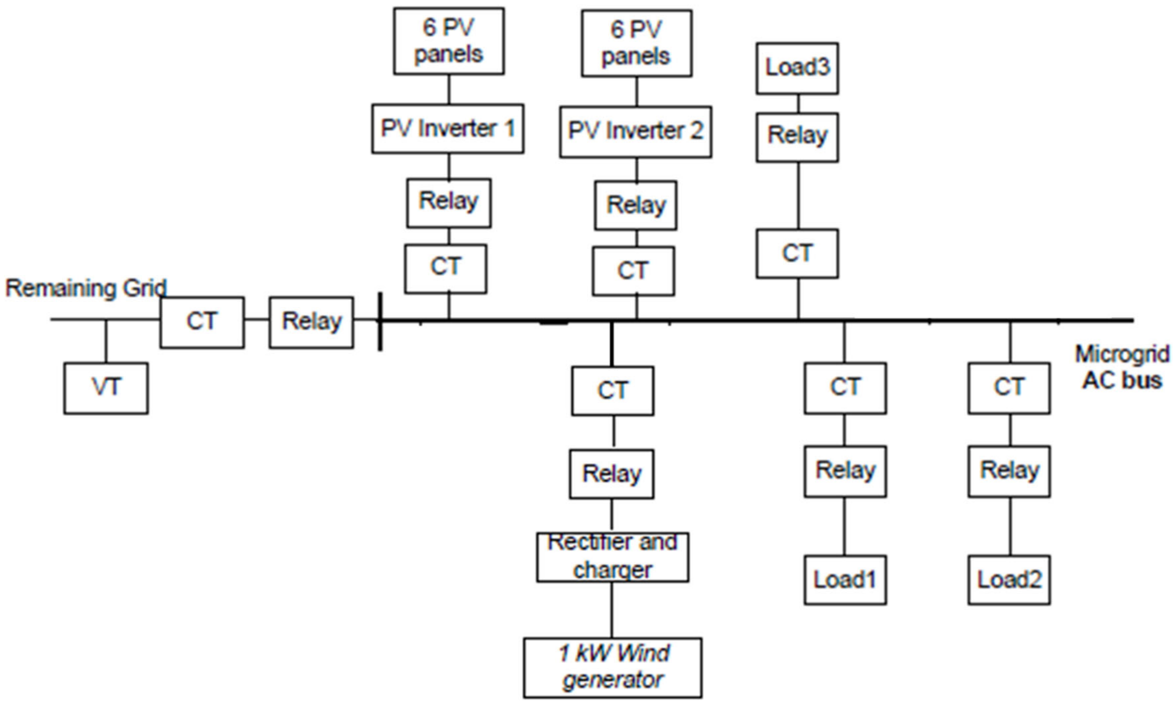

Figure 1. Implementation of a smart distribution grid topology.

The microgrid is made up of two 1.1 kW PV-inverters with six connected PV panels each and three loads with a maximum consumption of approximately 1500 W (1 AC-motor, incandescent lamps), as they are shown in Table 1.

Table 1. Lab appliance types.

Component	Load/Source Type	Rating
PV modules	Source	2 kW
Light 1	Managed load	250 W
Light 2	Managed load	250 W
Heating/cooling pump	Managed load	1 kW

2.1. Interoperability with KNX System

In this paper we have installed some KNX devices: a KNX power supply 160 mA, a switch on/off actuator of two channels, a dimmer actuator of four channels, an energy multi-tariff meter of three channels, a basic weather station, a push button with room temperature control, a presence detector with light control, and a KNX server for the visualization.

The KNX server (HomeLynk from Schneider Electric, Rueil-Malmaison, France) is required to incorporate KNX bus technologies into real-time measurements and decision systems in general. In the case of the experimental microgrid, in addition to the KNX devices the KNX HomeLynk server, as illustrated in Figure 2, should be installed on the microgrid. Load 1 in Figure 2 represents the motor (heating/cooling pump), while Load 2 and Load 3 represent a 500 W incandescent light group.

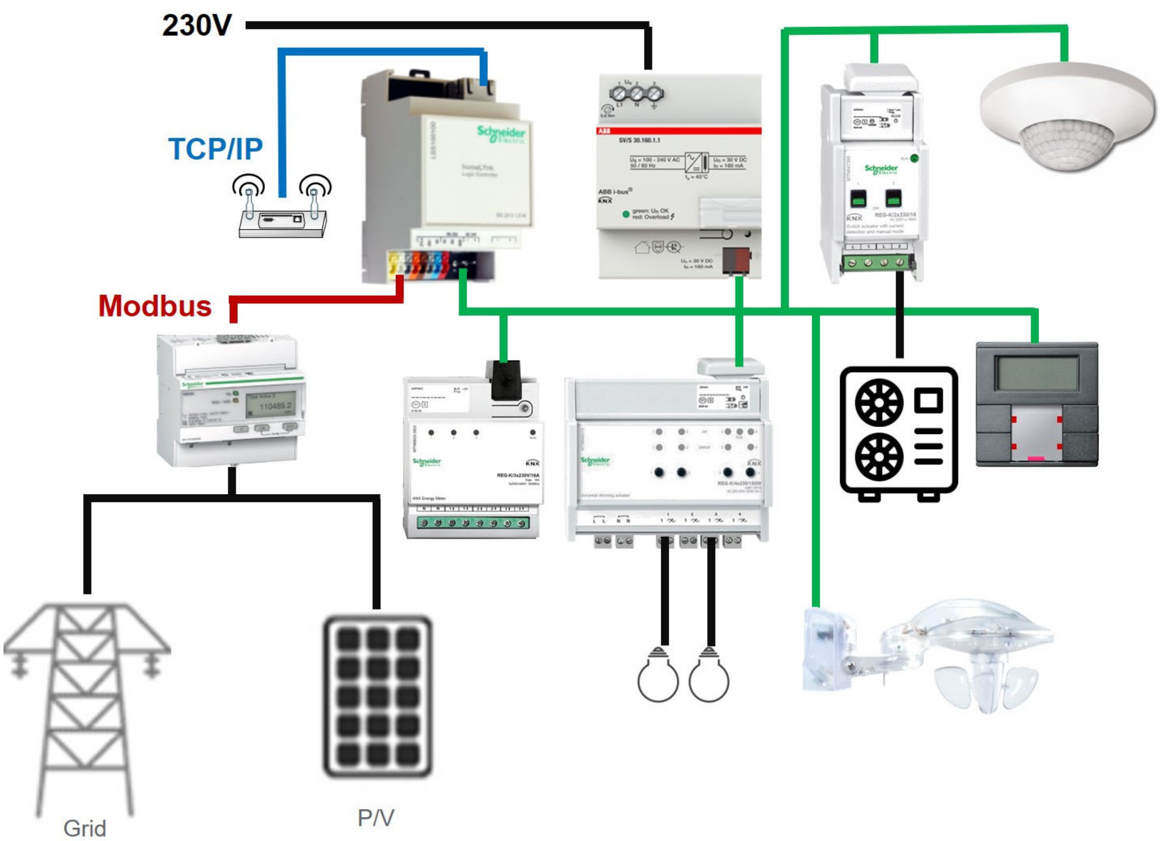

Figure 2. diagram of the BMS.

The BMS checks the PV energy, the real time energy price, and the average energy price through the multi-tariff energy meter continuously every 15 min. Recent smart homes provide room occupants with several options. According to this study, the optimal schedule of occupant rooms, i.e., the comfort zone, is defined and suggested to homeowners. The system checks the internal and external brightness of the room, the room temperature, the photovoltaic energy flow according to the weather prediction, the electricity real time price, and the average electricity price According to all these parameters the system dims the light up or down in the room, changes the temperature setpoint, and activates heating or cooling and the electric vehicle (EV) charge station.

2.2. Cost Effective Demand Side-Management

As previously stated, a simple and low-cost alternative option for integrating KNX-controlled loads into the microgrid control strategy is devised. KNX is the global standard for all building and smart city application control.

The majority of KNX-compatible load control devices are activated by KNX switches as well as traditional push buttons, the manipulations of which can be converted into binary signals. When the push button on a KNX dimmer is pressed briefly, the signal is translated into a pulse in the dimming mechanism. The inbuilt KNX program in the gadget transforms this pulse to full power for the lamps, and the lamps consume full power. On the other hand, sustained switch pressure indicates that the KNX device receives 1 bit signals sequentially. In this situation, the device begins lowering the voltage of the lamps until the pressing stops or the voltage is reduced to the final value set by the dimmer's original program. The lights and electricity usage are both lowered. If the button is held down for an extended period of time, the brightness is increased, and so on.

There are two main scenarios according to the flow chart in Figure 3. In scenario 1 the photovoltaic energy is greater than the demand energy, while in scenario 2 the photovoltaic energy is less than the demand power, and the real time electricity price is greater than the average electricity price. In scenario 3 the photovoltaic energy is less than the demand energy, and the real time electricity price is less than the average electricity price.

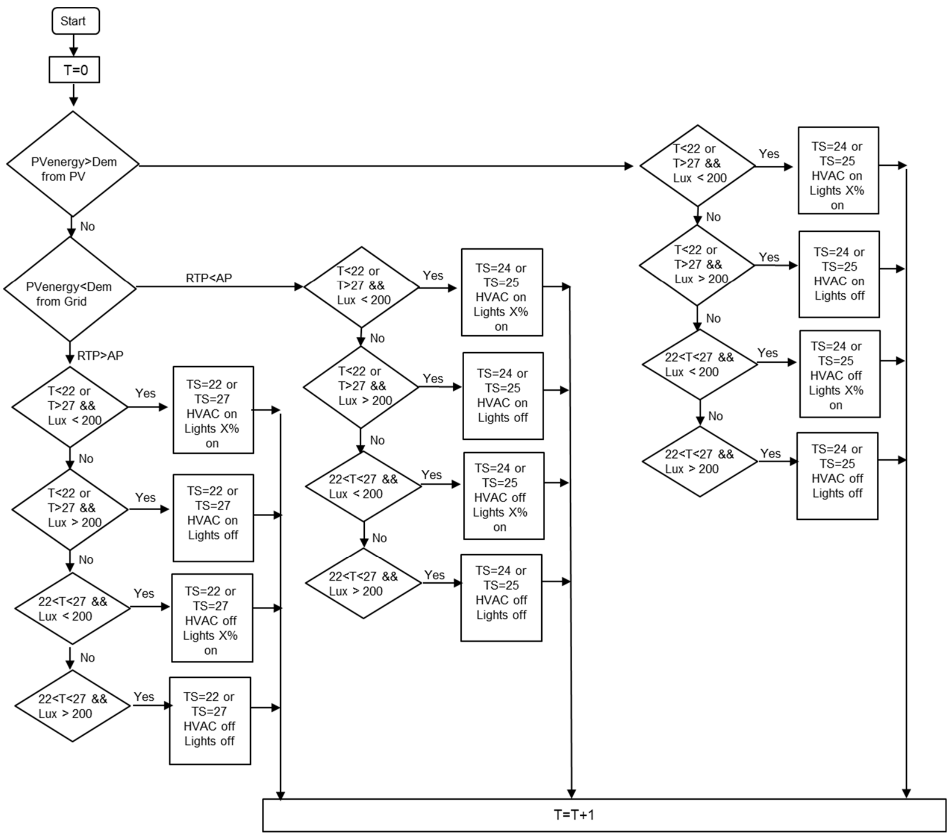

Figure 3. HomeLynk flow chart algorithm.

When the photovoltaic power is greater than the demand power, then the power source is the photovoltaic; otherwise, the power source is the grid.

The technical features of the multi-tariff energy meter are presented below in Table 2.

Table 2. Multi-tariff energy meter characteristics.

Direct measurement (up to 63 A)	Yes
Active Energy measurements	Yes
Four Quadrant Energy measurements	Yes
Electrical measurements (I, V, P, . . .)	Yes
Multi-tariff (internal clock)	4 inputs
Multi-tariff (controlled by digital inputs)	2 inputs
Measurement display	Yes
Digital inputs	1 input
Programmable digital outputs	1 input
Overload alarm	Yes
Modbus communication	Yes
MID (legal metrology certification)	Yes

The control algorithm's inputs are real-time measurements that are updated by the HomeLynk at each duty cycle and output variables that are supplied back into the iterative control method at the end of its execution period.

The algorithm's real-time measurement inputs are:

- the PV energy
- the signal for multi-tariffs
- the L1 energy in channel 1 of the dimmer
- the L2 energy in channel 1 of the dimmer
- the motor (heating/cooling) energy
- the internal lux in the lab
- the external lux
- the room temperature
- the room temperature setpoint

2.3. The HomeLynk Algorithm

The HomeLynk algorithm is presented in Figure 3. PV energy is the energy from photovoltaic panels, Dem is the demand energy, T is the room temperature, TS is the temperature setpoint, L is the internal brightness, REP is the real time energy price, and AP is the average energy price. There are many factors that can affect room temperature. The task of the algorithm control is to detect the actual temperature constantly and to ensure that the heating or cooling system receives new information accordingly. The heating or cooling system converts this information and adjusts the room temperature to the preconfigured setpoints. The actual temperature is continuously measured by the temperature sensor integrated into the push-button. The algorithm can control the connected heating/cooling systems via continuous correcting variables for the PI control. For the PI control, the correcting variable is calculated from a proportional and an integral share. The calculation is governed by parameters such as the temperature difference between the actual value and setpoint, proportional range, and reset time.

In this way, the controller can correct the room temperature quickly and accurately. With the switching PI control, also known as the PWM control, the correcting variables calculated by the controller (0–100%) are converted into a pulse–width modulation (PWM). Within a constant, defined cycle time, the control actuator is opened ("1") and then closed again ("0") for the calculated percentage period. For example, when a correcting variable of 25% is calculated for a cycle time of 12 min, a "1" is transmitted at the beginning of the cycle time, and a "0" is transmitted after three minutes (=25% of 12 min).

When the setpoint temperature changes, the controller calculates the required correcting variable and transmits it still within the current cycle (broken line).

The steps of the flow chart of the algorithm in Figure 3 is explained in more details, as follows:

- The photovoltaic energy is greater than the demand energy, the room temperature is less than 22 °C (winter) or greater than 27 °C (summer), and the internal brightness is less than 200 lux; then, the energy source is the PV, the temperature setpoint is 24 °C (winter) or 25 °C (summer), the heating/cooling pump is on, and the lamps L1 and L2 are dimmed up at X% brightness as follows: internal brightness + X% brightness = 200 lux.
- The photovoltaic energy is greater than the demand energy, the room temperature is less than 22 °C (winter) or greater than 27 °C (summer), and the internal brightness is greater than 200 lux; then, the energy source is the PV, the temperature setpoint is 24 °C (winter) or 25 °C (summer), the heating/cooling pump is on, and the lamps L1 and L2 are switched off.
- The photovoltaic energy is greater than the demand energy, the room temperature is greater than 22 °C (winter) or less than 27 °C (summer), and the internal brightness is less than 200 lux; then, the energy source is the PV, the temperature setpoint is 24 °C (winter) or 25 °C (summer), and the switching on and off of the heating/cooling pump depends on the current temperature. The lamps L1 and L2 are dimmed up at X% brightness as follows: internal brightness + X% brightness = 200 lux.
- The photovoltaic energy is greater than the demand energy, the room temperature is greater than 22 °C (winter) or less than 27 °C (summer), and the internal brightness is greater than 200 lux; then, the energy source is the PV, the temperature setpoint is 24 °C (winter) or 25 °C (summer), and the switching on and off of the heating/cooling pump depends on the current temperature. The lamps L1 and L2 are switched off.
- The photovoltaic energy is less than the demand energy, the real time energy price is greater than the average price, the room temperature is less than 22 °C (winter) or greater than 27 °C (summer), and the internal brightness is less than 200 lux; then, the energy source is the grid, the temperature setpoint is 22 °C (winter) or 27 °C (summer), the heating/cooling pump is on, and the lamps L1 and L2 are dimmed up at X% brightness as follows: internal brightness + X% brightness = 200 lux.
- The photovoltaic energy is less than the demand energy, the real time energy price is greater than the average price, the room temperature is less than 22 °C (winter) or greater than 27 °C (summer), and the internal brightness is greater than 200 lux; then, the energy source is the grid, the temperature setpoint is 22 °C (winter) or 27 °C (summer), the heating/cooling pump is on, and the lamps L1 and L2 are switched off.
- The photovoltaic energy is less than the demand energy, the real time energy price is greater than the average price, the room temperature is greater than 22 °C (winter) or less than 27 °C (summer), and the internal brightness is less than 200 lux; then, the energy source is the grid, the temperature setpoint is 22 °C (winter) or 27 °C (summer), the heating/cooling pump is on, and the lamps L1 and L2 are dimmed up at X% brightness as follows: internal brightness + X% brightness = 200 lux.
- The photovoltaic energy is less than the demand energy, the real time energy price is greater than the average price, the room temperature is greater than 22 °C (winter) or less than 27 °C (summer), and the internal brightness is greater than 200 lux; then, the energy source is the grid, the temperature setpoint is 22 °C (winter) or 27 °C (summer), the heating/cooling pump is on, and the lamps L1 and L2 are switched off.
- The photovoltaic energy is less than the demand energy, the real time energy price is less than the average price, the room temperature is less than 22 °C (winter) or greater than 27 °C (summer), and the internal brightness is less than 200 lux; then, the energy source is the grid, the temperature setpoint is 24 °C (winter) or 25 °C (summer), the heating/cooling pump is on, and the lamps L1 and L2 are dimmed up at X% brightness as follows: internal brightness + X% brightness = 200 lux.
- The photovoltaic energy is less than the demand energy, the real time energy price is less than the average price, the room temperature is less than 22 °C (winter) or greater than 27 °C (summer), and the internal brightness is greater than 200 lux; then, the

energy source is the grid, the temperature setpoint is 24 °C (winter) or 25 °C (summer), the heating/cooling pump is on, and the lamps L1 and L2 are switched off.

- The photovoltaic energy is less than the demand energy, the real time energy price is less than the average price, the room temperature is greater than 22 °C (winter) or less than 27 °C (summer), and the internal brightness is less than 200 lux; then, the energy source is the grid, the temperature setpoint is 24 °C (winter) or 25 °C (summer), the switching on and off of the heating/cooling pump depends on the current temperature. The lamps L1 and L2 are dimmed up at X% brightness as follows: internal brightness + X% brightness = 200 lux.
- The photovoltaic energy is less than the demand energy, the real time energy price is less than the average price, the room temperature is greater than 22 °C (winter) or less than 27 °C (summer), and the internal brightness is greater than 200 lux; then, the energy source is the grid, the temperature setpoint is 24 °C (winter) or 25 °C (summer), and the switching on and off of the heating/cooling pump depends on the current temperature. The lamps L1 and L2 are switched off.

The change of the temperature setpoint from 22 °C to 24 °C (winter), or from 27 °C to 25 °C, when the real time energy price is less than the average energy price leads to energy efficiency and to a reduction in the energy cost. In Greece the average energy price for homes is 0.18 €/Kwh, while the real time energy price is between 0.06 €/Kwh and 0.12 €/Kwh.

3. Results

The results show that none of the loads is totally rejected when the KNX automation system is used for load control actions instead of traditional on–off control [29]. In this paper we present the results of the HomeLynk server trends application in a single day in summer when the environmental temperature is 35 °C. Figure 4 shows the low and the high electricity price during the day. As one can see, the low-price periods are 24:00–06:00, 15:00–17:00 and 19:00–24:00. In the remaining time during the day there is a high electricity price. In the next two Figures (Figures 5 and 6) we present the temperature setpoint and the room temperature. As one can see, in the low-price periods the temperature setpoint is 25 °C, and in the high-price periods the temperature setpoint increases automatically to 27 °C.

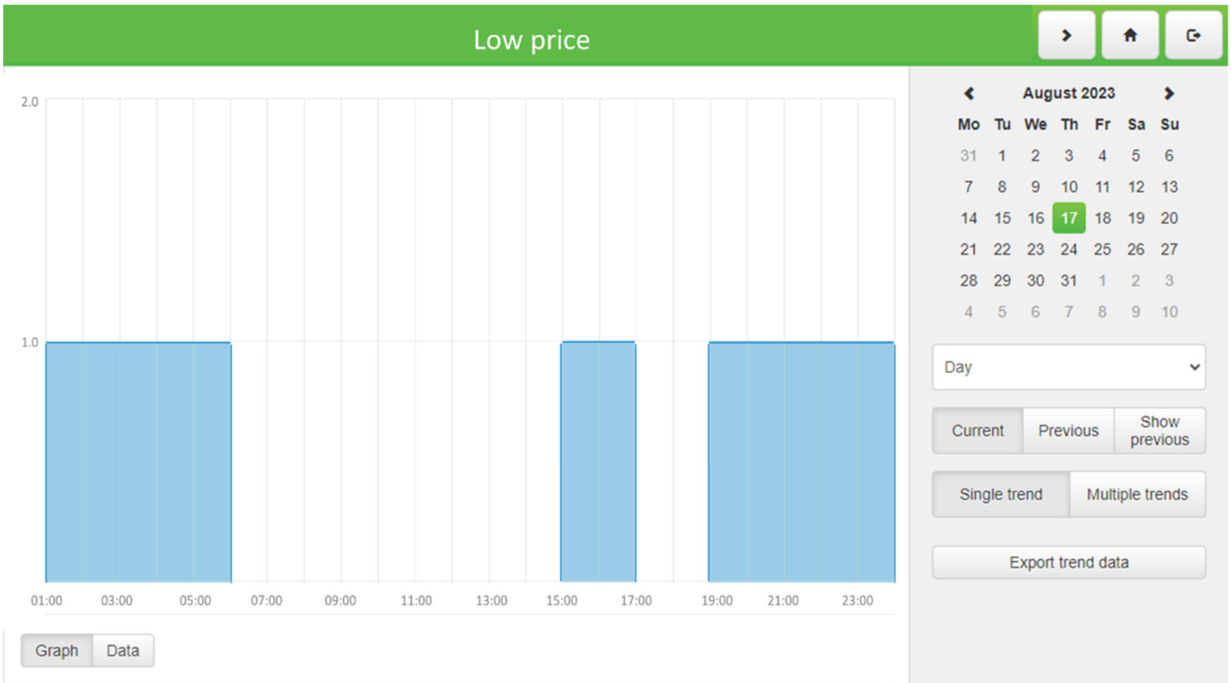

Figure 4. Low price signal.

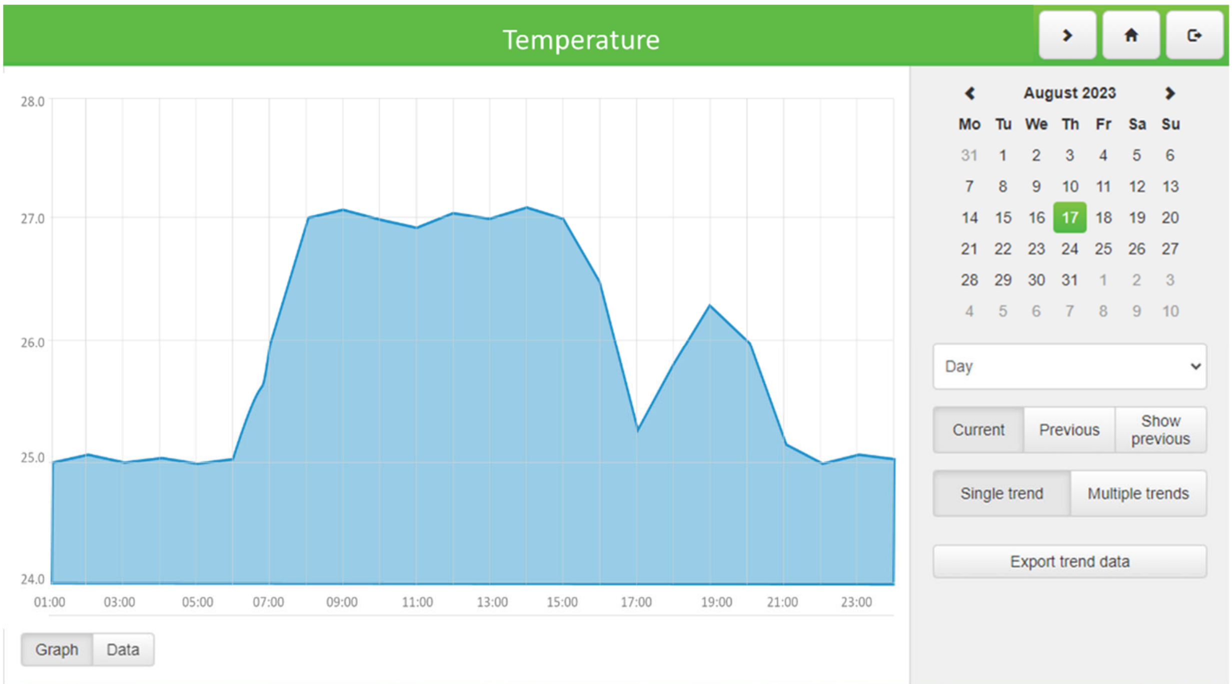

Figure 5. Room temperature.

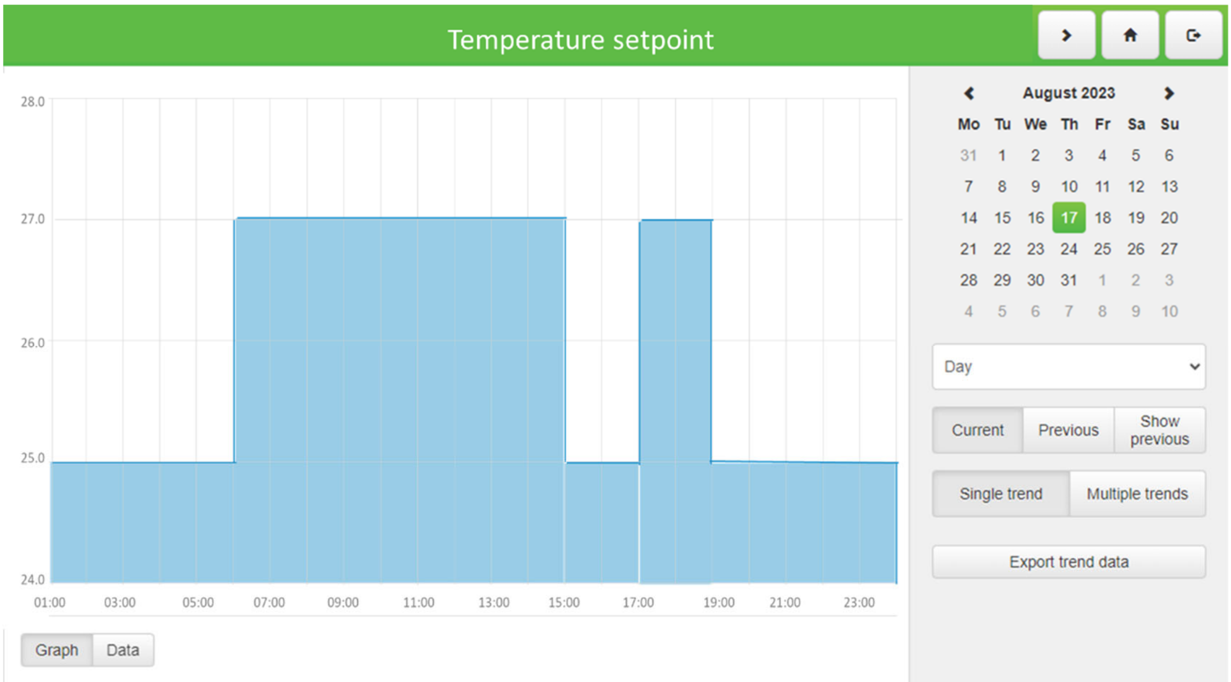

Figure 6. Room setpoint temperature.

In the next five Figures (Figures 7–11) we present the room internal brightness according to the external brightness, the brightness of the lamps L1 and L2, and the energy consumption of the lamps L1 and L2. The lamps L1 and L2 are dimmed up. During the low-price periods, if the total room brightness is less than 200 lux the lamps are dimmed up at X% brightness as follows: internal brightness + X% brightness = 200 lux.

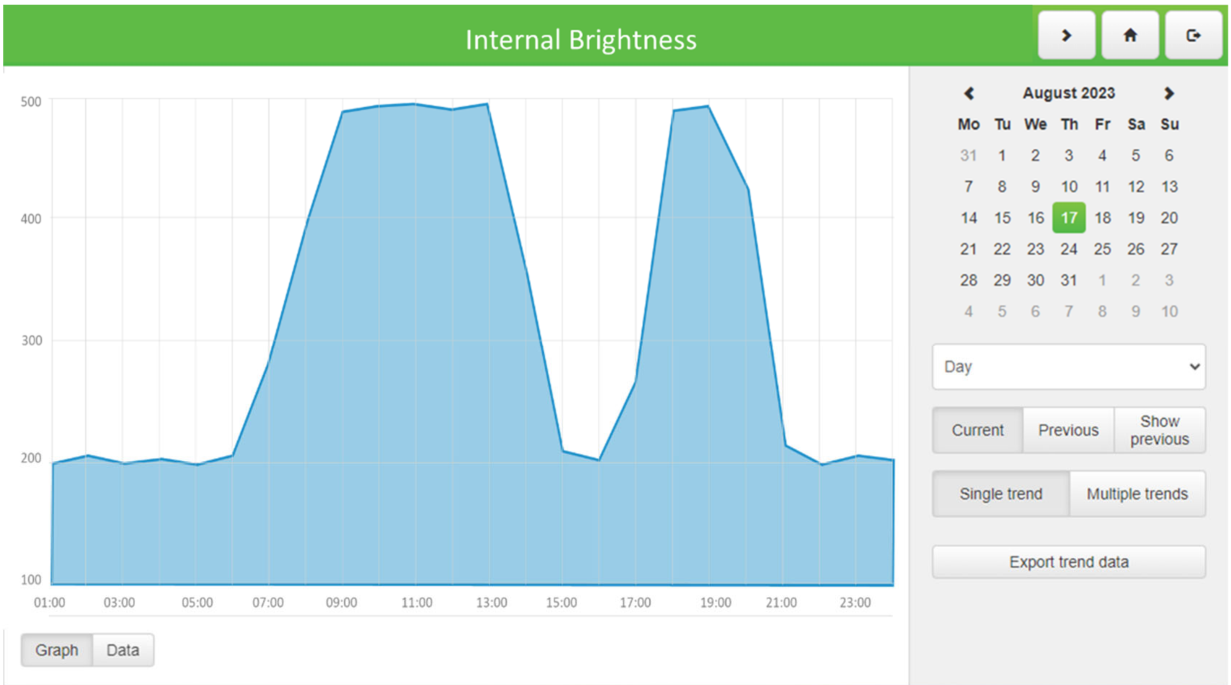

Figure 7. Room internal brightness.

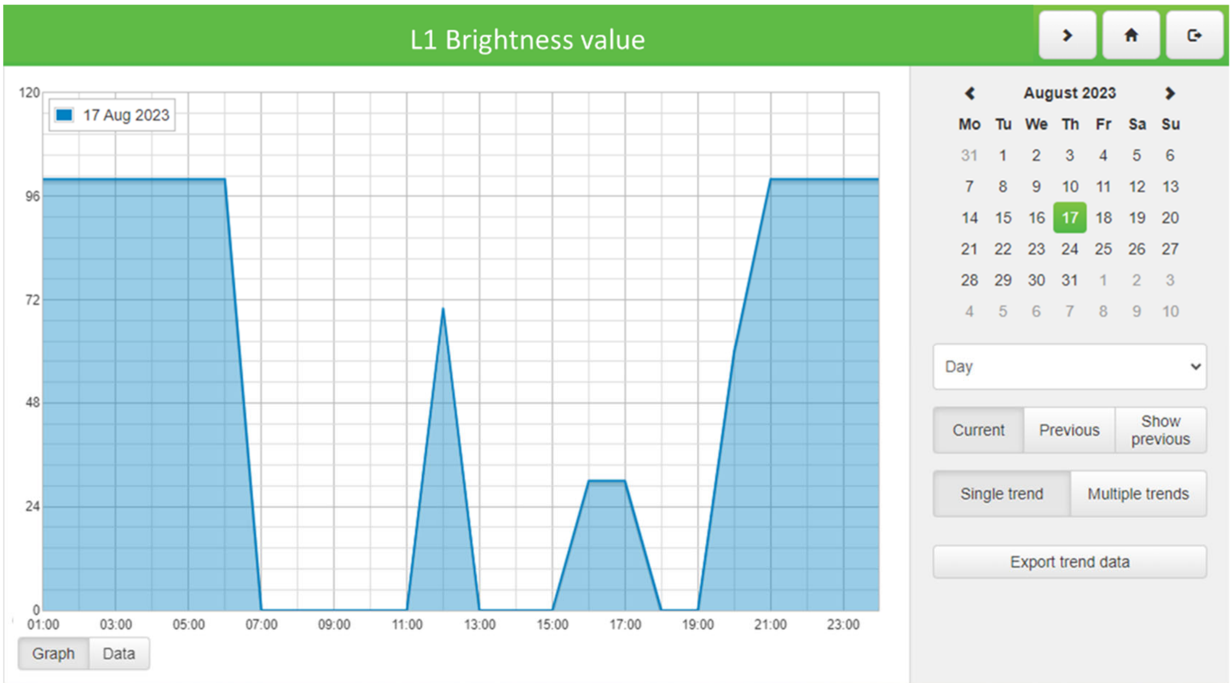

Figure 8. L1 brightness value.

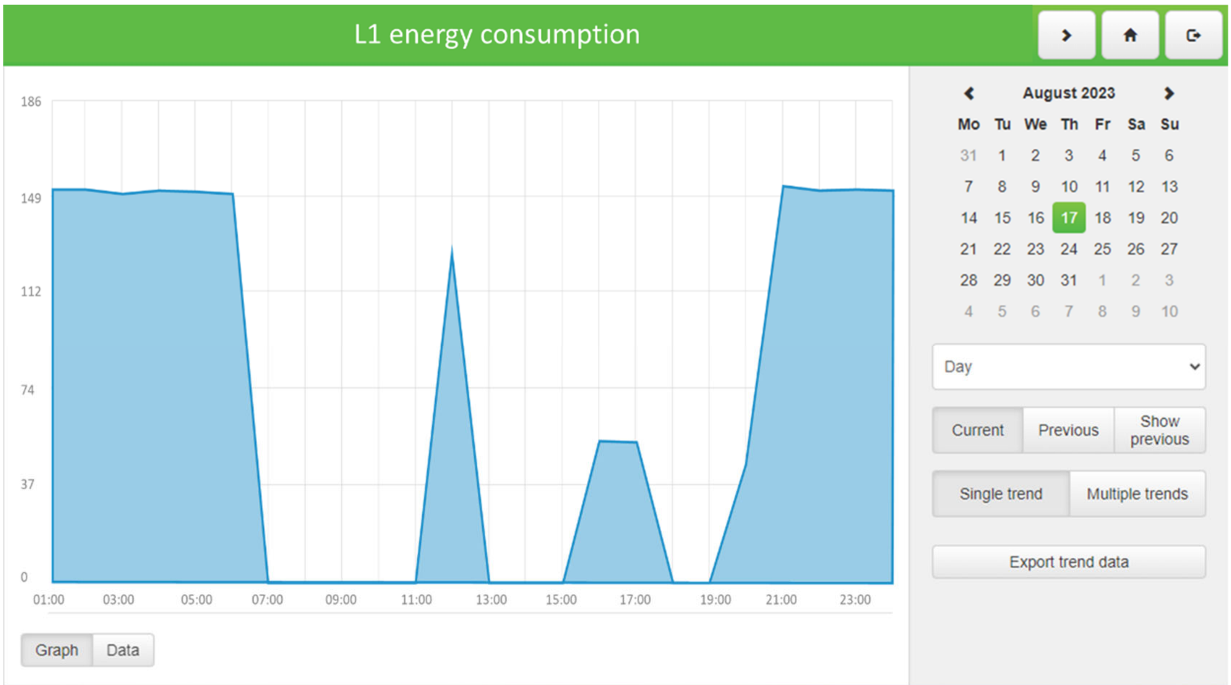

Figure 9. L1 energy consumption.

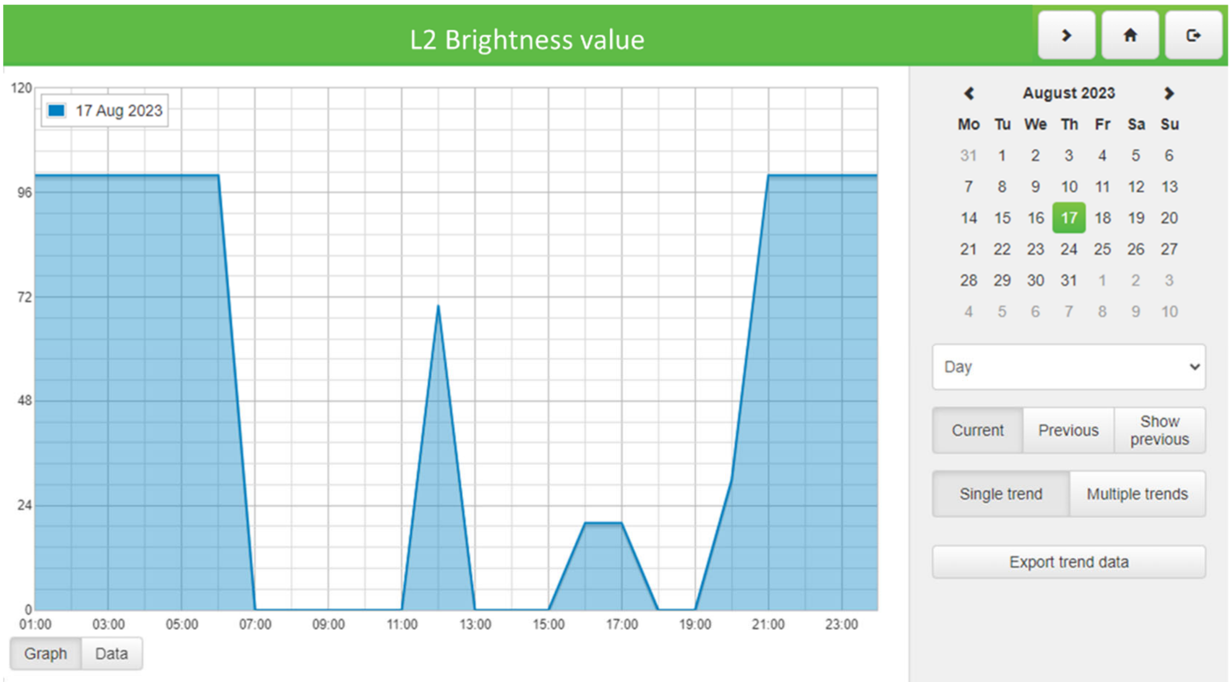

Figure 10. L2 brightness value.

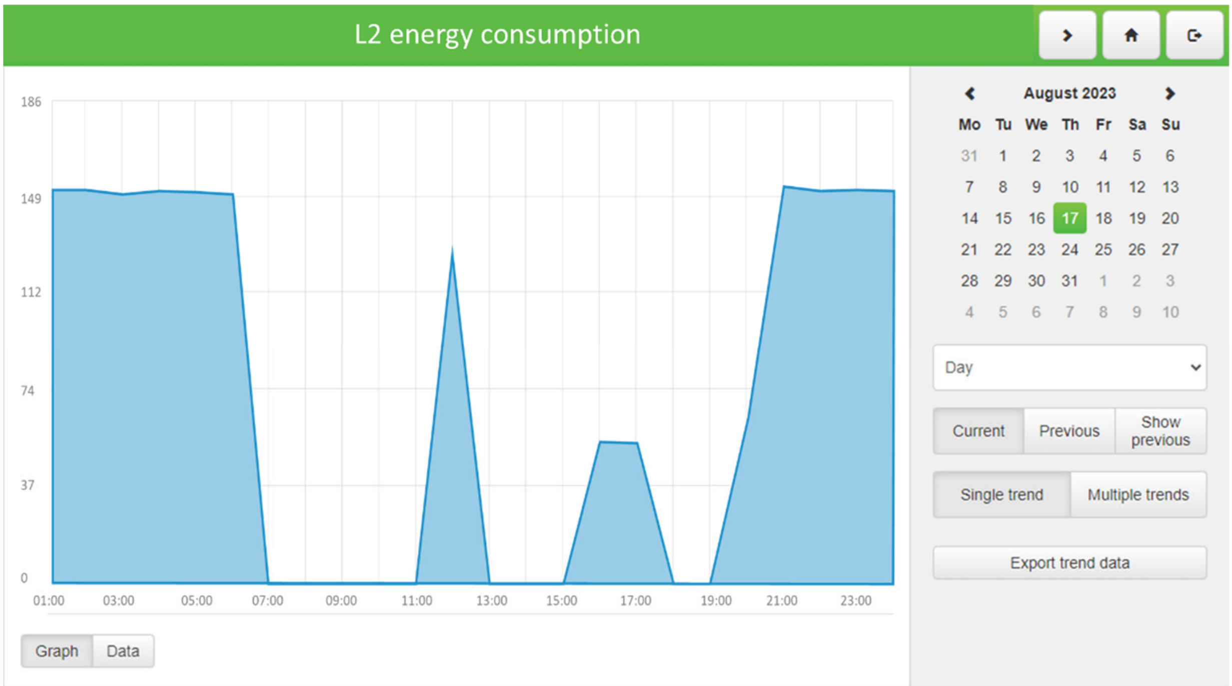

Figure 11. L2 energy consumption.

Figure 12 below shows heating/cooling pump energy consumption, while Figure 13 presents the motor energy consumption in comparison to the room setpoint temperature, and the room temperature according to the low price.

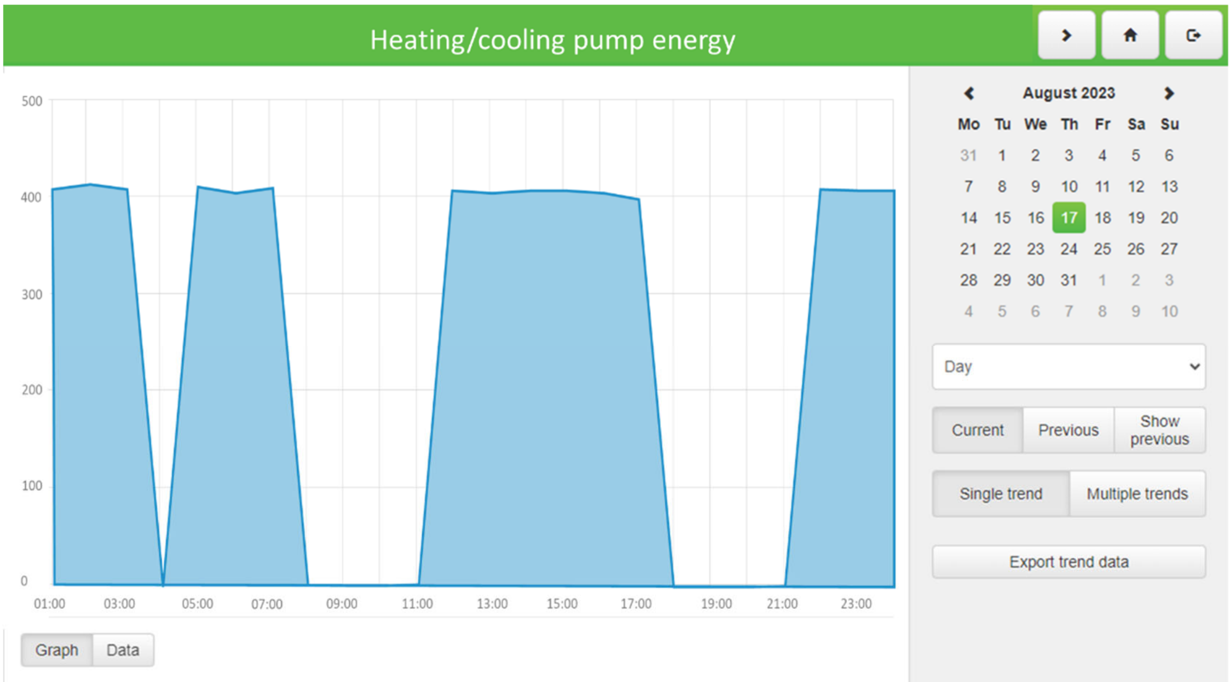

Figure 12. Heating/cooling pump energy consumption.

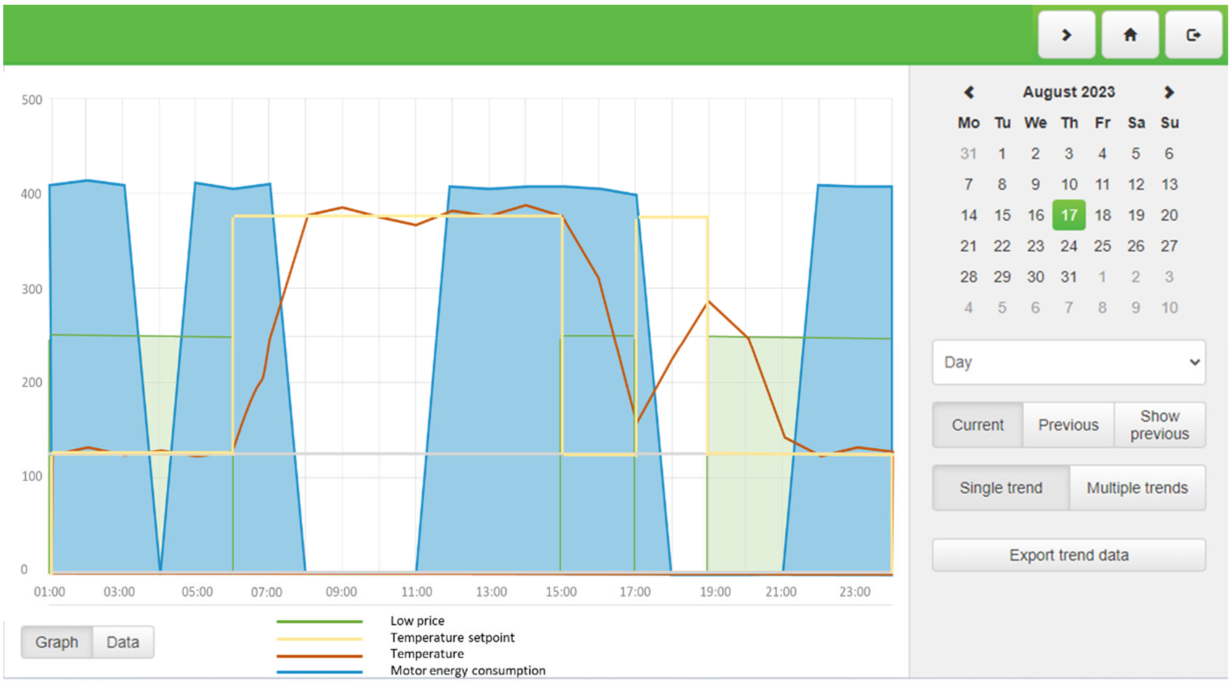

Figure 13. Low price, room temperature, setpoint temperature, and heating/cooling pump energy consumption.

In Table 3 the results of the first experiment are presented.

Table 3. Results during the day with average room temperature 25.89 °C.

Hours	Temperature °C	Energy Consumption Wh
01:00	25	403
02:00	25	406
03:00	25	403
04:00	25	405
05:00	25	403
06:00	25	403
07:00	25.7	404
08:00	27	0
09:00	27	0
10:00	27	0
11:00	27	0
12:00	27	403
13:00	27	406
14:00	27	403
15:00	27	405
16:00	26.5	403
17:00	25.3	405
18:00	25.7	0
19:00	26.2	0
20:00	26	0
21:00	25.1	0
22:00	25	405
23:00	25	403
24:00	25	405
Average	25.89	217.88

After these results a second experiment is conducted without the low-price signal and the HomeLynk algorithm. According to this, the energy consumption is presented in

Figure 14, when the setpoint temperature is always 26 °C during the day. In Table 4 the results of the second experiment are presented.

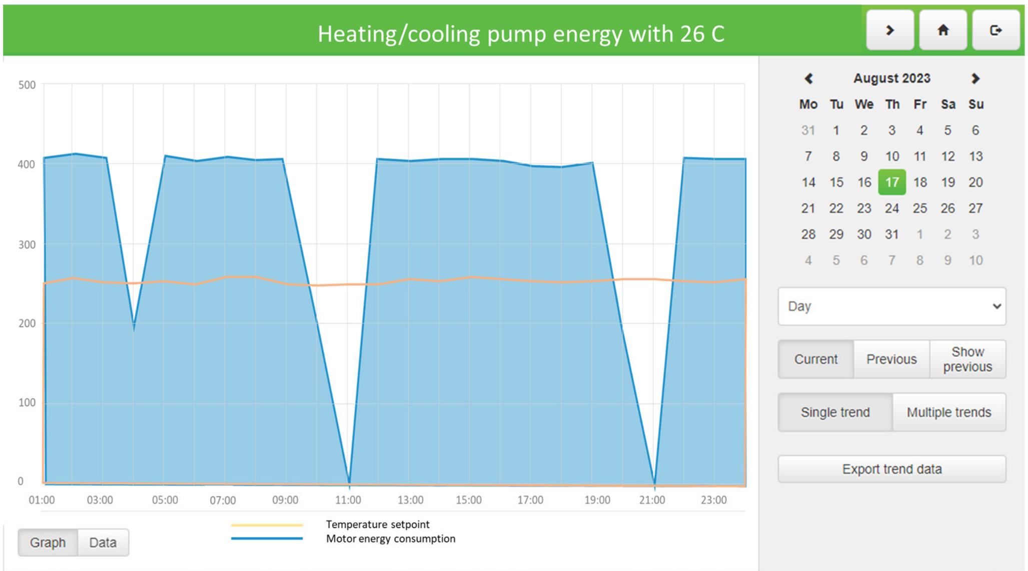

Figure 14. Heating/cooling pump energy consumption with temperature setpoint at 26 °C.

Table 4. Results during the day with average room temperature 26 °C.

Hours	Temperature °C	Energy Consumption Wh
01:00	26	403
02:00	26	406
03:00	26	403
04:00	26	205
05:00	26	405
06:00	26	403
07:00	26	407
08:00	26	403
09:00	26	405
10:00	26	203
11:00	26	0
12:00	26	403
13:00	26	406
14:00	26	403
15:00	26	405
16:00	26	403
17:00	26	405
18:00	26	403
19:00	26	406
20:00	26	196
21:00	26	403
22:00	26	405
23:00	26	403
24:00	26	405
Average	26	361.91

By comparing Tables 3 and 4, the suggested system transfers the selected load (heating/cooling pump) to a time with low electricity prices, and the total energy consumption is 217.88 Wh with an average room temperature of 25.89 °C, instead of 361.91 Wh with an average temperature of 26 °C.

Taking into account only the energy consumption of the heating/cooling pump and an average environmental temperature in the summer of 35 °C, the monthly energy cost savings are too high. The total monthly energy consumption is lowered to 6536.4 Wh instead of 10,857 Wh, reducing by 40%.

The suggested BMS schedules the lab appliances based on the tariff category, which changes based on the total accumulated usage during the day. The proposed BMS takes two major factors into account in order to provide a comfortable lifestyle for users. Users can change the ambient temperature to their favorite region. Recent smart homes allow for a variety of room inhabitants. The best schedule of inhabitant rooms, i.e., the comfort zone, is determined and advised to homeowners. The area covered by a heating/cooling pump (chiller) is simply adjusted to minimize energy consumption by designating comfort zones, i.e., a room/rooms that vary depending on the available tariff category. Second, all appliances can be switched on and off manually to satisfy the sudden wants of home residents.

4. Discussion

The next steps of the research include the integration of energy storage (14.4 kWh batteries and 2 hydrogen fuel cells of 1.1 kWs each) into the microgrid, which will also be controlled by KNX decentralized algorithms, highlighting the impact of energy storage in grid stability and grid ancillary services indices, as well as comfort indices. Installing a battery will probably increase the economic benefits of the home PV system. Vehicle-to-home will also be studied as an alternative source for smart homes. Therefore, there will be the economic benefit of using electric vehicle batteries as a home source with the studied slab tariff.

5. Conclusions

Many developing countries, including Greece, use IBR tariffs for residential structures or "homes." There have been no significant studies on this popular tariff in relation to smart homes.

The suggested BMS relies primarily on a load-shifting technique, which moves controllable loads to low-cost periods to avoid high loading during peak hours. The paper proposes a residential DR optimization model that coordinates the benefits of households and utility operators. The model aims to minimize the individual household electricity consumption cost while considering customers' comfort and lifestyle.

Many BMS minimize some loads, such as heating/cooling pumps and lighting, to reduce total spent energy. All of these options were investigated for the IBR pricing structure.

To perform the proposed approach, the thermal comfort-based control algorithm for a heating system in the BMS was proposed to improve the ocupants' thermal comfort. At the same time, a dimming lighting system (LED) was integrated into the visual comfort-based control algorithm of the lighting system in the BMS to improve the visual comfort and energy savings of the household.

The results showed that the heating system with PWM-based control significantly improved the thermal comfort of the occupants during both the DR and non-DR periods, as well as the energy consumption, compared to the heating system with switching on/off. In addition, the visual comfort based on illuminance and energy savings of a lighting system controlled by the proposed approach in the BMS was also validated. The total monthly cost was reduced to 40% of the default value.

This research looks at a developing country's household energy system that uses the Greek block-rate tariff.

In the future, the proposed BMS can be implemented in large buildings such as town halls, schools, hospitals, etc. Greece already participates in many Interreg Europe projects (Greece–Albania, Greece–Cyprus, Greece–Skopje) and more specifically in the call for energy efficiency in buildings. We have already installed this BMS in the town hall of Igoumenitsa, and we will publish it in a future paper.

Author Contributions: Conceptualization, C.S.; methodology, C.S.; software C.S.; validation, D.T. and D.S.; formal analysis, C.S.; investigation, C.S.; resources, D.S.; data curation, C.S.; writing—original draft preparation, D.T.; writing—review and editing, C.S.; visualization, C.S.; supervision, D.S.; project administration, C.S.; funding acquisition, D.T. All authors have read and agreed to the published version of the manuscript.

Funding: This research was funded by the Operational Programme "Competitiveness, Entrepreneurship and Innovation" (NSRF 2014-2020) and co-financed by Greece and the European Union (European Regional Development Fund). The APC was funded by the Operational Programme "Competitiveness, Entrepreneurship and Innovation" (NSRF 2014-2020) and co-financed by Greece and the European Union (European Regional Development Fund). Information regarding the funder and the funding number should be provided under the project with RESCOM code 80579 of the Research Committee of the University of Western Macedonia and also supported by the project: "Development of New Innovative Low-Carbon Energy Technologies to Enhance EXCELlence in the Region of Western Macedonia" (MIS 5047197) under the Action "Reinforcement of the Research and Innovation Infrastructure", funded by the Operational Programme "Competitiveness, Entrepreneurship and Innovation" (NSRF 2014-2020) and co-financed by Greece and the European Union (European Regional Development Fund).

Data Availability Statement: Data is unavailable due to privacy reasons.

Conflicts of Interest: The authors declare no conflict of interest.

References

1. Laaksonen, H.; Kauhaniemi, K.; Voima, S. Microgrid voltage level managementand role as part of smart grid voltage control. In Proceedings of the IEEE PowerTech 2011, Trondheim, Norway, 19–23 June 2011.
2. *European Technical Standard EN 15232*; Energy Performance of Buildings—Impact of Building Automation, Control, and Building Management. Comité Européen de Normalisation: Brussels, Belgium, 2012. Available online: http://www.cres.gr/greenbuilding/PDF/prend/set4/WI_22_TC-approval_version_prEN_15232_Integrated_Building_Automation_Systems.pdf (accessed on 20 December 2020).
3. The European Parliament and the Council of the European Union. *Directive 2010/31/EU of the European Parliament and of the Council of 19 May 2010 on the Energy Performance of Buildings*; The European Parliament and the Council of the European Union: Brussels, Belgium, 2010. Available online: https://eurlex.europa.eu/LexUriServ/LexUriServ.do?uri=OJ:L:2010:153:0013:0035:en:PDF (accessed on 20 December 2020).
4. Roadmap, E.C.F. 2050 Project. Available online: http://www.roadmap2050.eu/ (accessed on 20 December 2020).
5. De Brabandere, K.; Vanthournout, K.; Driesen, J.; Deconinck, G.; Belmans, R. Controlof microgrids. In Proceedings of the IEEE Power Engineering Society General Meeting, Tampa, FL, USA, 24–28 June 2007.
6. Meliopoulos, A.P.; Cokkinides, G.; Huang, R.; Farantatos, E.; Choi, S.; Lee, Y.; Yu, X. Smart grid technologies for autonomous operation and control. *IEEE Trans. Smart Grids* **2011**, *2*, 1–10. [CrossRef]
7. Shoreh, M.H.; Siano, P.; Shafie-Khah, M.; Loia, V.; Catalão, J.P.S. A survey of industrial applications of Demand Response. *Electr. Power Syst. Res.* **2016**, *141*, 31–49. [CrossRef]
8. Eissa, M.M. Developing incentive demand response with commercial energy management system (CEMS) based on diffusion model, smart meters and new communication protocol. *Appl. Energy* **2019**, *236*, 273–292. [CrossRef]
9. Samuel, O.; Javaid, S.; Javaid, N.; Ahmed, S.H.; Afzal, M.K.; Ishmanov, F. An efficient power scheduling in smart homes using jaya based optimization with time-of-use and critical peak pricing schemes. *Energies* **2018**, *11*, 3155. [CrossRef]
10. Du, Y.F.; Jiang, L.; Li, Y.; Wu, Q. A robust optimization approach for demand side scheduling considering uncertainty of manually operated appliances. *IEEE Trans. Smart Grid* **2018**, *9*, 743–755. [CrossRef]
11. Javaid, N.; Ahmed, A.; Iqbal, S.; Ashraf, M. Day ahead real time pricing and critical peak pricing-based power scheduling for smart homes with different duty cycles. *Energies* **2018**, *11*, 1464. [CrossRef]
12. Huang, Y.; Wang, L.; Guo, W.; Kang, Q.; Wu, Q. Chance constrained optimization in a home energy management system. *IEEE Trans. Smart Grid* **2018**, *9*, 252–260. [CrossRef]
13. Shafie-Khah, M.; Siano, P. A stochastic home energy management system considering satisfaction cost and response fatigue. *IEEE Trans. Ind. Inf.* **2018**, *14*, 629–638. [CrossRef]
14. Dinh, H.T.; Kim, D. An optimal energy-saving home energy management supporting user comfort and electricity selling with different prices. *IEEE Access* **2021**, *9*, 9235–9249. [CrossRef]
15. Dinh, H.T.; Yun, J.; Kim, D.M.; Lee, K.-H.; Kim, D. A home energy management system with renewable energy and energy storage utilizing main grid and electricity selling. *IEEE Access* **2020**, *8*, 49436–49450. [CrossRef]
16. Makhadmeh, S.N.; Khader, A.T.; Al-Betar, M.A.; Naim, S.; Abasi, A.K.; Alyasseri, Z.A.A. A novel hybrid grey wolf optimizer with min-conflict algorithm for power scheduling problem in a smart home. *Swarm Evol. Comput.* **2021**, *60*, 100793. [CrossRef]

17. Makhadmeh, S.N.; Khader, A.T.; Al-Betar, M.A.; Naim, S.; Abasi, A.K.; Alyasseri, Z.A.A. Optimization methods for power scheduling problems in smart home: Survey. *Renew. Sustain Energy Rev.* **2019**, *115*, 109362. [CrossRef]
18. Lee, S.; Choi, D.H. Energy management of smart home with home appliances, energy storage system and electric vehicle: A hierarchical deep reinforcement learning approach. *Sensors* **2020**, *20*, 2157. [CrossRef] [PubMed]
19. Park, H.; Rhee, S.B. IoT-based smart building environment service for occupants' thermal comfort. *J. Sens.* **2018**, *2018*, 1757409. [CrossRef]
20. Li, M.; Li, G.Y.; Chen, H.R.; Jiang, C.W. QoE-aware smart home energy management considering renewable and electric vehicles. *Energies* **2018**, *11*, 2304. [CrossRef]
21. Laaksonen, H.; Saari, P.; Komulainen, R. Voltage and frequency control of inverter based weak LV network microgrid. In Proceedings of the International Conference of Future Power Systems, Amsterdam, The Netherlands, 18 November 2005; pp. 1–6.
22. Brabandere, K.D.; Woyte, A.; Belmans, R.; Nijs, J. Prevention of inverter volt-age tripping in high density PV grids. In Proceedings of the 19th Photovoltaic Solar Energy Conference, Paris, France, 7–11 June 2004.
23. Kottas, T.; Stimoniaris, D.; Tsiamitros, D.; Kikis, V.; Boutalis, Y.; Dialynas, E. New operation scheme and control of smart grids using fuzzy cognitive networks. In Proceedings of the IEEE Power Tech 2015 Conference, Eindhoven, The Netherlands, 29 June–2 July 2015; pp. 1–5.
24. Zehir, M.A.; Batman, A.; Bagriyanik, M. An event-driven energy management system for planned control of thermostatic loads. In Proceedings of the IEEE Power Tech 2013 Conference, Grenoble, France, 16–20 June 2013.
25. Vandoorn, T.L.; Renders, B.; Degroote, L.; Meersman, B.; Vandevelde, L. Active load control in islanded microgrids based on the grid voltage. *IEEE Trans. Smart Grids* **2011**, *2*, 139–151. [CrossRef]
26. Piller, S.; Perrin, M.; Jossen, A. Methods for state-of-charge determination and their applications. *J. Power Sources* **2001**, *96*, 113–120. [CrossRef]
27. Sunny Island Installation Guide, Version 4.0. Available online: http://www.sma.de (accessed on 21 August 2023).
28. Stimoniaris, D.; Tsiamitros, D.; Poulakis, N.; Kottas, T.; Kikis, V.; Dialynas, E. Investigation of smart grid topologies using pilot installations-experimental results. In Proceedings of the IEEE-ISGT-2011, Manchester, UK, 5–7 December 2011.
29. Tsiamitros, D.; Stimoniaris, D.; Poulakis, N.; Zehir, M.A.; Batman, A.; Bagriyanik, M.; Dialynas, E. Advanced energy storage and demand-side management in smart grids using buildings energy efficiency technologies. In Proceedings of the IEEE Innovative Smart Grid Technologies 2014 Conference (IEEE-ISGT2014), Istanbul, Turkey, 12–15 October 2014.
30. Stimoniaris, D.; Tsiamitros, D.; Dialynas, E. Improved Energy Storage Management and PV-Active Power Control Infrastructure and Strategies for Microgrids. *IEEE Trans Power Syst.* **2016**, *31*, 813–820. [CrossRef]
31. KNX—The International Buildings Control and Automation Standard. Available online: www.knx.org (accessed on 21 August 2023).
32. Langhammer, N.; Kays, R. Performance evaluation of wireless home automation networks in indoor scenarios. *IEEE Trans. Smart Grids* **2012**, *3*, 2252–2261. [CrossRef]
33. Aliberti, M. Green networking in home and building automation systems through power state switching. *IEEE Trans. Consum. Electron.* **2011**, *57*, 445–452. [CrossRef]
34. Zehir, M.A.; Batman, A.; Sonmez, M.A.; Font, A.; Tsiamitros, D.; Stimoniaris, D.; Kol-latou, T.; Bagriyanik, M.; Ozdemir, A.; Dialynas, E. Development of a field data-based virtual test bed for microgrid integration of building automation technologies. In Proceedings of the ELECO 2015 Conference, Bursa, Turkey, 26–28 November 2015.